1950 *Macromolecules* **2010**, *43*, 1950–1957
DOI: 10.1021/ma902459a

Macromolecules
ARTICLE

Temperature-Induced, Reversible Swelling Transitions in Multilayers of a Cationic Triblock Copolymer and a Polyacid

Wui Siew Tan,[†] Robert E. Cohen,[‡] Michael F. Rubner,*[,†] and Svetlana A. Sukhishvili*[,§]

[†]*Department of Materials Science and Engineering, and* [‡]*Department of Chemical Engineering, Massachusetts Institute of Technology, 77 Massachusetts Avenue, Cambridge, Massachusetts 02139, and* [§]*Department of Chemistry, Chemical Biology and Biomedical Engineering, Stevens Institute of Technology, Hoboken, New Jersey 07030*

Received November 6, 2009; Revised Manuscript Received December 18, 2009

ABSTRACT: In this article, we seek to enable large-scale, fully reversible, thermally induced volumetric changes in layer-by-layer (LbL) electrostatically self-assembled thin films through the incorporation of A-B-A triblock copolymers. Poly(*N*,*N*-dimethylaminoethyl methacrylate)-*b*-poly(propylene oxide)-*b*-poly(*N*,*N*-dimethylaminoethyl methacrylate) (abbreviated "PD-PPO-PD") was used as a dual pH and temperature-responsive component in the electrostatic self-assembly of multilayer thin films. In solutions of this triblock copolymer with poly(*N*,*N*-dimethylaminoethyl methacrylate) (PD) weak polyelectrolyte end blocks, the dehydration temperature of the central poly(propylene oxide) (PPO) block was strongly dependent on solution pH, as shown by microdifferential scanning calorimetry (micro-DSC) and dye solubilization techniques. Multilayer films were then assembled with poly(acrylic acid) (PAA) or poly(4-styrene sulfonate) (PSS) as anionic binding partners at various pH values, where the triblock copolymer was incorporated within the film either as unimers or micelles. Using in situ ellipsometry, we showed that the polyanion type and the self-assembly pH were both critical parameters for constructing functional films, which change their swelling degree in response to temperature. In particular, strongly associated PD-PPO-PD/PSS multilayers lacked temperature sensitivity and maintained a constant swelling degree in a wide range of pH and temperature. In contrast, the temperature response of PD-PPO-PD/PAA films was strongly dependent on the self-assembly pH. Whereas swelling of PD-PPO-PD/PAA films constructed at pH $\leq$ 5 was independent of temperature, multilayers assembled at pH $\geq$ 6 showed fully reversible, three- to five-fold changes in film thickness in response to temperature cycling between 6 and 20 °C, enabled by the ability of PPO domains to transit reversibly between the swollen hydrated and collapsed dehydrated states. These nanocomposite coatings show highly responsive, reversible swelling transitions that can be useful for future biomedical and device applications.

1. Introduction

Materials that respond to environmental changes or enable triggered, on-demand responses by the application of a suitable stimulus (such as light, temperature, pH, or salt concentration) are promising for a range of biomedical and micromechanical device applications. In particular, for biological systems where pH is often limited to a narrow range of values, temperature, as opposed to pH control, provides a convenient means of externally triggered response. There has been considerable effort to develop responsive materials that change dimensions,[1−3] mechanical properties,[4,5] wettability,[6−9] and permeability[10−12] with temperature. To achieve the desired thermal responsiveness, polymers that undergo reversible temperature-dependent hydration in aqueous environments have been studied; examples include poly(*N*-substituted acrylamides), poly(*N*-vinyl alkylamides), poly(vinyl ethers), and poly(ethylene oxide-*co*-propylene oxide).[13−17] These polymers have traditionally been utilized as covalently cross-linked water-swellable bulk materials. However, the macroscopic dimensions of these polymerized gels result in slow response kinetics, which may restrict their potential applications. To circumvent these limitations, several studies have focused on reducing the dimensions of these materials and creating thin film coatings of thermally responsive polymers.

*To whom correspondence should be addressed. E-mail: rubner@mit.edu (M.F.R.); ssukhish@stevens.edu (S.A.S.).

Layer-by-layer (LbL) assembly by sequential adsorption of components that interact via electrostatics,[18] hydrogen bonding,[19] or specific chemical reaction[20] has proven to be a facile method that can create conformal coatings, of several angstroms to micrometers thick, on a variety of substrates.[18] Major benefits of this technique are the ability to employ all-aqueous processing, to control nanometer-scale thicknesses, to customize the molecular composition, and to introduce porosity into thin film coatings. By applying the LbL technique to sacrificial template colloid materials, one can also easily create hollow capsules.[21,22] Temperature- or pH-responsive capsules have thus been created via LbL assembly.[23−25] To confer LbL multilayers with temperature sensitivity, a temperature-responsive component is incorporated. One of the first approaches to create temperature-responsive thin film hydrogels via the LbL method was demonstrated by Serizawa et al. and involved sequential reactions between poly(vinylamine-*co*-*N*-vinylisobutyramide) and poly(acrylic acid) (PAA) on a gold surface.[26] Subsequently, electrostatically assembled multilayers were created by Steitz et al. using a diblock of poly(4-styrene sulfonate)-*b*-poly(N-isopropylacrylamide) (PSS-*b*-PNIPAM) and polycations.[27] Glinel et al. reported the creation of hollow thermoresponsive multilayer capsules of similar diblock copolymers.[28] However, in these reports, the response of the LbL films to temperature was irreversible. Reversible but limited to acidic conditions, swelling of electrostatically assembled LbL films of PNIPAM-*co*-PAA microgels with poly(allylamine hydrochloride) (PAH) was reported by Serpe et al.[29] These

 Published on Web 01/21/2010

temperature-responsive microgel multilayers demonstrated thermally triggered release of insulin[30] and doxorubicin[31] at acidic pH values. Recently, Jaber and Schlenoff documented the reversible uptake and release of water from electrostatically self-assembled multilayers of random copolymers PNIPAM-*co*-PSS and PNIPAM-*co*-PAH with corresponding changes in multilayer permeability.[32] Hydrogen-bonded (H-bonded) LbL assembly of temperature-responsive polymers is another viable route to create temperature-responsive films. Several possible H-bonded systems are described by Kharlampieva et al.[33] Quinn and Caruso demonstrated the use of a PNIPAM and PAA H-bonded system to load and release a hydrophobic dye with temperature cycling,[34] whereas most recently, Zhu et al. demonstrated the temperature-induced swelling and small molecule release from hydrogen bonded poly(*N*-vinylpyrrolidone)-*b*-PNIPAM micelles and poly(methacrylic acid) (PMAA).[35] Furthermore, the stability of H-bonded multilayers containing temperature-responsive homopolymers (such as PNIPAM) has been found to be temperature-dependent. The dissolution of these H-bonded multilayers below a critical temperature has been used to harvest micrometer-sized patches of patterned polyelectrolyte multilayers[36] and studied in detail for application as temperature-triggered release films.[37] One limitation of hydrogen-bonded films is their pH stability, which is limited to pH values below the pK_a of the H-bond donor.

Here we report on temperature-responsive LbL films that contain electrostatically assembled triblock copolymers and demonstrate temperature-triggered swelling transitions in a wide range of pH. To the best of our knowledge, the incorporation of triblock copolymers into polyelectrolyte multilayers for temperature-controlled dimensional changes has yet to be reported. This strategy offers a new avenue to confer novel and useful properties to LbL assemblies. We demonstrate that the use of an A-B-A triblock copolymer with charged end-blocks A and a thermoresponsive middle-block B provides large, well-defined, and reversible dimensional changes of the film with temperature. Separation of binding and response functions between the end blocks and the central block of the A-B-A triblock copolymer is ideal for achieving two key functions of responsive multilayers. First, in such configuration, the temperature response properties, defined by the length and character of the central block, are conserved and not "diluted" by a random distribution of hydrophilic charged monomer units, which would raise the lower critical solution temperature (LCST) of the copolymer[38] and form ionic cross-links within electrostatically assembled films, both of which would compromise the temperature response of this unit. Second, the central B block of the A-B-A triblock copolymer, capable of collapsing in response to temperature variations, is able to transmit effectively this contraction throughout the electrostatically bound network because it is structurally fixed within the film by attachment through charged A blocks at both ends. We describe the use of a symmetric A-B-A triblock copolymer; PD-*b*-PPO-*b*-PD (abbreviated "PD-PPO-PD") to create reversibly temperature-responsive multilayers. PPO exhibits LCST behavior and its temperature-dependent solubility in water as a part of copolymers is best documented within the family of nonionic di- and triblock copolymers of poly(ethylene glycol) (PEO) and PPO commonly known as poloxamers and commercialized under the trade name Pluronic.[39−44] PD-PPO-PD is an interesting polyelectrolyte analogue of the well-known PEO-*b*-PPO-*b*-PEO triblock copolymers, which should have similar phase- and temperature-responsive properties based on the central PPO block of similar molecular weight. Armes and coworkers have done significant work on the synthesis and solution characterization of various different PD-containing di-, tri-, and terblock copolymers,[45−49] whereas the solution pH and temperature sensitivity of PD-PPO-PD in particular has been reported by other groups.[50,51] Here we present the use of a triblock copolymer with charged anchoring end blocks to create electrostatically assembled multilayers with broad pH stability and large amplitude, fully reversible swelling and deswelling temperature responsive properties. We show that the multilayers' temperature response is critically dependent on both the assembly conditions and the choice of anionic binding partner for electrostatic self-assembly. These findings demonstrate that the incorporation of triblock copolymers into multilayer films is an effective means to include nanoscopic domains with partitioning, reactive, or stimuli responsive functions through selection of an appropriate central block.

2. Materials and Methods

2.1. Materials. Poly(acrylic acid) (PAA, $M_w \geq 200\,000$ g/mol; 25% aqueous solution) from Polysciences, poly(4-styrene sulfonate) (PSS, $M_w \approx 70\,000$) from Sigma-Aldrich, poly(*N*,*N*-dimethylaminoethyl methacrylate)-*b*-poly(propylene oxide)-*b*-poly(*N*,*N*-dimethylaminoethyl methacrylate), PD-PPO-PD ($M_w \approx 1600-3000-1600$) triblock copolymers from Polymer Source, and 1,6-diphenyl-1,3,5-hexatriene (DPH) from Sigma Aldrich were used as received.

2.2. Multilayer Construction. For building of multilayers, we used 10^{-2} M solutions (based on the repeat unit molecular weight) of PAA or PSS polyanions and 0.1 mg/mL solutions of PD-PPO-PD polycation in deionized, ultrapure Millipore water with resistivity 18 MΩ·cm (abbreviated as "DI" henceforth). The pH of all polymer solutions and the DI rinse solutions were adjusted to the desired dipping pH by the addition of 1 M NaOH or 1 M HCl. Substrates used were polished ⟨100⟩ silicon wafers purchased from Wafernet. Wafers were first UV irradiated for 2 h, rinsed in DI water, dried, and further cleaned using 150 mTorr oxygen plasma (PDC-32G, Harrick Scientific Products) for 30 min. All multilayer thin films were assembled at room temperature (RT) (of ∼24 °C) by an automated StratoSequence VI spin dipper (from nanoStrata), controlled by StratoSmart v6.2 software, with substrates spun at 130−160 rpm. The dipping time in each polymer solution was 10 min followed by three rinse steps (of 2, 1, and 1 min) in DI water adjusted to the same pH as that of the polymer solutions used. The nomenclature for PEM films follows the convention ("polycation"/"polyanion" $Y)_Z$, where Y represents the pH of the polycation, polyanion, and DI water rinse solutions used during assembly, and Z is the total number of bilayers (polycation + polyanion) deposited. Because the substrates used have an originally negative surface potential, the first component deposited is the polycation and integral values of Z indicate that the PEM was finished with a polyanion deposition step.

2.3. Spectroscopic Ellipsometry. Thicknesses and refractive indices were measured using a Woollam VASE spectroscopic ellipsometer. Data were collected between 300 and 1000 nm at a 70° incidence angle and analyzed with WVASE32 software package. Data were fitted with a Cauchy model, which assumes the real part of the refractive index, n_f, as a function of wavelength, λ, to be $n_f(\lambda) = A_n + B_n/\lambda^2 + C_n/\lambda^4$, where A_n, B_n, and C_n are fitted constants. Film thicknesses were also independently confirmed (to be within 10%) using a P16 (KLA-Tencor Corporation) surface profiler. For in situ ellipsometry swelling measurements, a home-built quartz cell was used to measure film thickness when immersed in aqueous solution, as described in a previous publication.[52] The refractive index of the pH-adjusted DI solutions was assumed to be that of water (1.33). Because the lateral dimensions of the substrate-bound thin films are constrained, the swelling ratio of the PEMs in solution was defined as the ratio of the swollen film thickness to dry film thickness.

2.4. Microdifferential Scanning Calorimetry (micro-DSC). Differential scanning calorimetry measurements were done using a Microcal MC-2 instrument (Microcal, Amherst, MA). DI or sample (1.5 mL) was used in Hastelloy reference or sample cell, respectively. Both reference and sample cells were sealed

during the measurements to prevent solvent evaporation at higher temperatures. Solutions of 3.3 mg/mL PD-PPO-PD were adjusted to pH 4, 5, 6, 6.5, 7, 7.5, 8, or 11.4 immediately prior to measurements. Temperature scans were performed at a ramp rate of 1 K/min. Cycles between 5 and 65 °C were repeated at least three times for each sample to ensure the reproducibility of the exothermic and endothermic temperature-induced transitions.

2.5. Dye Solubilization. A stock solution of 0.4 mM DPH in methanol and, separately, PD-PPO-PD solutions of 1 and 0.1 mg/mL in DI were adjusted to pH 4, 7, and 8. DPH/methanol solution (15 μL) was added to 1.5 mL of the PD-PPO-PD solution to obtain a 0.004 mM solution of DPH in 1% v/v methanol/water. Samples were poured in Teflon-stoppered disposable plastic UV-transparent cuvettes with a path length of 1 cm and left in the dark to equilibrate at 6 °C for 2 h before spectroscopic measurements. Using the method described by P. Alexandridis et al.,[53] the absorption spectra of the copolymer/DPH/water samples were recorded in the 300−500 nm range using a Varian, Cary 500i UV−vis-NIR dual-beam spectrophotometer, equipped with a temperature controller connected to an electrothermal multicuvette holder. The temperature range of 6−40 °C was scanned with a heating rate of 0.06 K/min. The peak absorption at 356 nm, characteristic of DPH, was recorded as a function of temperature.

2.6. Dynamic Light Scattering. The number-average hydrodynamic diameter of PD-PPO-PD unimers and micelles in solution at various pH and temperature was determined using ZetaPals (Brookhaven Instrument) with temperature control and particle sizing functions.

3. Results and Discussion

3.1. Temperature-Triggered Micellization of PD-PPO-PD in Solution. *3.1.1. Effects of pH.* Prior to depositing PD-PPO-PD within multilayer films, we studied the solution properties of PD-PPO-PD to determine its temperature-dependent hydration as a function of solution pH and ionic strength. We used two techniques: micro-DSC and a dye solubilization technique. Micro-DSC is a well-documented method used to determine the LCST of polymer solutions[54] and study temperature-dependent micellization[55] or thermally induced collapse and aggregation of block copolymers.[56,57] For di- and triblock copolymers containing 1.6−4 kDa PPO blocks, a range of micellization temperatures (MTs) between 5 and 50 °C[53,58] have been reported. Because PD has a LCST of ∼75 °C for solutions at pH 7,[59] solutions were not heated above 65 °C to avoid precipitation of the polymers. In micro-DSC experiments, an endothermic event associated with PPO dehydration and aggregation was observed during heating, and a corresponding exothermic event associated with PPO hydration, and dissolution occurred during cooling. Because the onset temperature of the thermal events was close to the lower temperature limit of the instrument in some cases, the MT was taken as the temperature at which peak heat flow was recorded during cooling. Although the cooling process corresponded to dissolution of micelles rather than micellization, this exothermic event was used to characterize the MT because it showed better reproducibility and more well-defined peaks. The aggregation and micellization process during heating gave broader and occasionally irregularly shaped peak regions that stretch across the same temperatures corresponding to the demicellization event registered during cooling. A representative heating and cooling curve obtained from microcalorimetric measurements of the triblock copolymer at 3.3 mg/mL in DI water adjusted to pH 7 is shown in Figure S1 of the Supporting Information.

Figure 1 shows that the MT of PD-PPO-PD was strongly dependent on pH. The MT decreased from 31 to 12 °C as the pH was increased from 4 to 11.4. As mentioned in the Introduction, PPO has been extensively studied as a part of di- and triblock copolymers with hydrophilic polymer blocks, namely, PEO. These amphiphilic block copolymers show rich composition, temperature, and concentration-dependent phase behavior[40,58,60] with micellization temperatures tunable between 5 and 50 °C.[53,58] Our data fall reasonably within this range of values. Unlike the end blocks of PEO-*b*-PPO-*b*-PEO, PD is a weak polybase with a variable charge density. When a weak polyelectrolyte (wPE) acquires additional charge, its crowding in the micellar corona becomes increasingly energetically unfavorable, and the increased barrier toward micellization is revealed in an increase in MT. Indeed, in our case (Figure 1), a sharp increase in MT from ∼13 to ∼30 °C occurred when pH was lowered from 7.5 to 6, that is, in the region close to the pK_a of PD of ∼6.7, as reported by others[61] and confirmed by us using potentiometric titration (data not shown). Our finding that the solution pH and ionization of the PD end blocks strongly influence PD-PPO-PD's ability to form micelles is consistent with the literature on other wPE block copolymers.[48,62−64] Above pH 7.5, the PD blocks in PD-PPO-PD were weakly ionized, and micellization occurred at ∼13 °C. At pH 6 and below, the high positive charge density on PD posed an energetic barrier to the formation of micelles, increasing the MT to ∼30 °C.

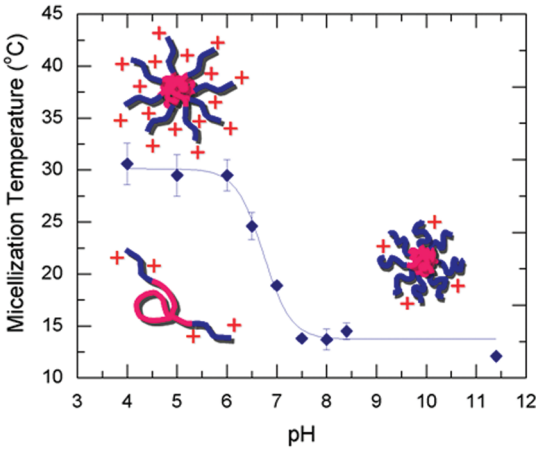

Figure 1. pH dependence of the micellization temperature in 3.3 mg/mL PD-PPO-PD solutions with no added salt. The MT was determined from the peak exotherm observed during cooling from 65 to 6 °C in micro-DSC experiments. Cartoons show the state of the polymer chains above and below the MT at the pH extremes.

The data on pH-dependent micellization of PD-PPO-PD was also confirmed using a dye solubilization technique; another established method to determine critical micelle concentration (CMC) and critical micellization temperature (CMT).[53] Absorption and fluorescence of DPH is minimal in water but increases significantly when DPH is incorporated into hydrophobic cores of micelles formed above the CMC or CMT. Following the protocol used by P. Alexandridis et al.,[53] the absorbance of PD-PPO-PD and dye solutions was recorded at 356 nm as a function of solution temperature, and the CMTs were obtained from the first break in the sigmoid curves showing an increase in absorbance with increasing temperature. (See Figure S2 in the Supporting Information.) Table 1 compares the CMT obtained from dye solubilization and the estimated MT from microDSC. The values for the MT obtained with the two different techniques agreed within 2 °C. From both the micro-DSC and dye solubilization data, we confirmed that in the absence of added salt in 0.1 mg/mL solutions of PD-PPO-PD at RT

Table 1. Micellization Temperatures of PD-PPO-PD Solutions at Different pH Obtained Using microDSC and DPH-Solubilization Techniques

solution pH	$MT_{micro\text{-}DSC}$ (°C)	$CMT_{dye\ solubilization}$ (°C)
4	30.5	30.0
7	18.0	16.5
8	13.5	12.0

of ~24 °C, the triblock copolymer was molecularly dissolved at pH ≤ 6, whereas it formed PPO-core/PD-corona micelles at pH ≥ 7.

Micellization and micelle sizes were also studied using dynamic light scattering (DLS) (Supporting Information, Figure S3). At temperatures below 10 °C, a number-average hydrodynamic diameter of ~6 nm was detected in PD-PPO-PD solutions at pH 4 and 7, consistent with the presence of unimers. In contrast, as the temperature was increased, the hydrodynamic size evolution drastically differed between pH 4 and 7 solutions. Whereas at pH 4, the small, unimer-like size of ~6 nm persisted up until 30 °C, a sharp increase in the number-average hydrodynamic diameter to ~19 nm occurred in PD-PPO-PD solutions at pH 7 at ~20 °C. As a lower bound theoretical estimate of the block copolymer dimensions, we calculated the radius of gyration (assuming θ conditions), $R_g = N^{0.5}\, b/6^{0.5}$, where N is the number of polymer segments and b is the segmental length. The hydrodynamic radius, $R_h = 0.66R_g$, and for our triblock copolymer ($N \approx 74$, $b \approx 0.33$ nm), the resulting hydrodynamic diameter, $D_h = 2R_h \approx 1.53$ nm. The experimentally obtained D_h at low pH (pH 4) is about 4 times higher because water is a good solvent for the PD end blocks, and electrostatic repulsions between DMA units cause further electrostatic chain extension. Above 20 °C at pH 7, the micellar diameter was ~19 nm, a reasonable size given that PD-PPO-PD has a contour length of 25 nm (assuming backbone C−C−O and C−O−C bond angles of 109.5 and 115°, respectively, together with characteristic bond lengths of 1.54 Å for C−C bonds and 1.43 Å for C−O bonds). The DLS-inferred MT of PD-PPO-PD indicated by the increase in hydrodynamic diameter was in good agreement with the micro-DSC and dye solubilization data.

3.1.2. Effects of Salt. To confirm that a high degree of ionization and electrostatic repulsions between PD end blocks was the key factor that contributed to the increased CMT of PD-PPO-PD at low pH values, we studied the effect of salt on PD-PPO-PD micellization. Figure S4 in the Supporting Information section shows that at pH 4, micellization of PD-PPO-PD in 0.2 M NaCl solutions occurred at ~19 °C instead of its original value of ~31 °C in the absence of added salt. This result showed that screening of charges in the PE block decreased the electrostatic repulsions between corona chains and lead to more facile micellization.

3.2. Multilayers of PD-PPO-PD with Polyanions. *3.2.1. Layer-by-Layer Assembly of PD-PPO-PD with PSS or PAA.* With an understanding of the pH and temperature-dependent solution behavior of PD-PPO-PD, we set out to determine how the two possible molecular states (unimer versus micelle) would influence the multilayer assembly process. All multilayers discussed in this article were assembled from aqueous solutions with no added salt and at room temperature of ~24 °C. Figure 2 shows the evolution of the dry ellipsometric film thickness from LbL assembly of PD-PPO-PD with PAA or PSS at pH 4 or 7. The film growth was dramatically dependent on the polyanion type used in the multilayer assembly (Figure 2). Whereas the PD-PPO-PD/PAA system exhibited exponential growth (at pH4) and a large increase in thickness with layer number, growth of the

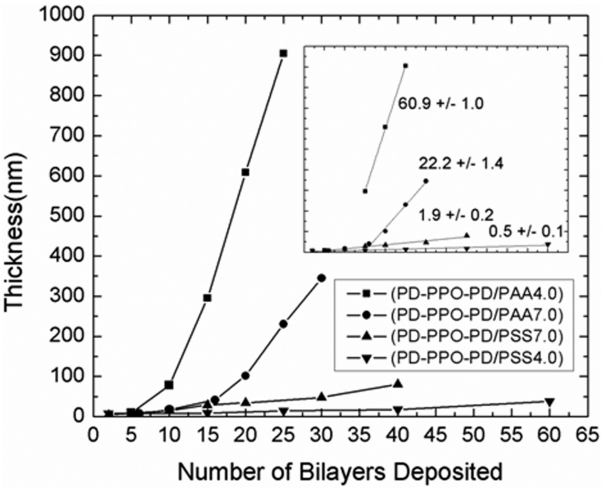

Figure 2. Thickness of multilayer assemblies as a function of the number of bilayers deposited from solutions without added salt at 24 °C. Inset shows the line fit to linear regions of each curve as well as the slope of the curve and standard error of the fit.

Table 2. Average Thickness Increment Per Bilayer for (PD-PPO-PD/PAA4.0)$_{15-25}$, (PD-PPO-PD/PSS4.0)$_{1-60}$, (PD-PPO-PD/PAA7.0)$_{16-30}$, and (PD-PPO-PD/PSS7.0)$_{1-40}$[a]

system	thickness per bilayer (nm)
(PD-PPO-PD/PAA4.0)$_{15-25}$	60.9
(PD-PPO-PD/PSS4.0)$_{1-60}$	0.5
(PD-PPO-PD/PAA7.0)$_{16-30}$	22.2
(PD-PPO-PD/PSS7.0)$_{1-40}$	1.9

[a] Subscripts indicate regions of linear film growth used to calculate the incremental bilayer thicknesses.

PD-PPO-PD/PSS multilayers was essentially linear with very small thickness increments per deposition cycle. Table 2 shows the average thickness increment per bilayer for each of the systems obtained from linear fits to regions of the growth curves shown in the inset of Figure 2.

3.2.1.1. Layer-by-Layer Assembly of PD-PPO-PD with PSS. In the case of the PD-PPO-PD/PSS multilayer system assembled at pH 4.0, the very low thickness increments are similar to what has been observed when two fully charged polyelectrolytes are assembled in the absence of added salt.[65] AFM studies done by Tsukruk et al.,[66] for example, have also shown that PSS adsorbs to positively charged surfaces as a smooth thin layer composed of highly flattened macromolecular chains. Because PSS is a strong polyelectrolyte, the PSS chains are fully charged and present a high negative surface charge density to the adsorbing PD-PPO-PD molecules that in turn adsorb in a flat outstretched manner. As such, the PD-PPO-PD/PSS4.0 multilayers consist of thin layers of PSS and PD-PPO-PD. It is interesting to note that the neutral central PPO block does not seem to influence significantly the growth behavior under these conditions. Unlike the PD-PPO-PD solution used at pH 4.0, at pH 7.0, the PD-PPO-PD solutions at room temperature (~24 °C) contain both positively charged micelles and unimers. (See Figure 1.) As a result of this difference, the PD-PPO-PD/PSS7.0 system had a larger thickness increment per bilayer than PD-PPO-PD/PSS4.0. Interestingly, compared with the thickness increment reported for LbL assembly of micelle−micelle multilayers, of 20−30 nm per layer of micelles deposited,[67] the bilayer thickness increment for the PD-PPO-PD/PSS7.0 film of 1.9 nm per bilayer is much lower and closer to that expected from LbL assemblies of non-micellar polyelectrolyte systems.

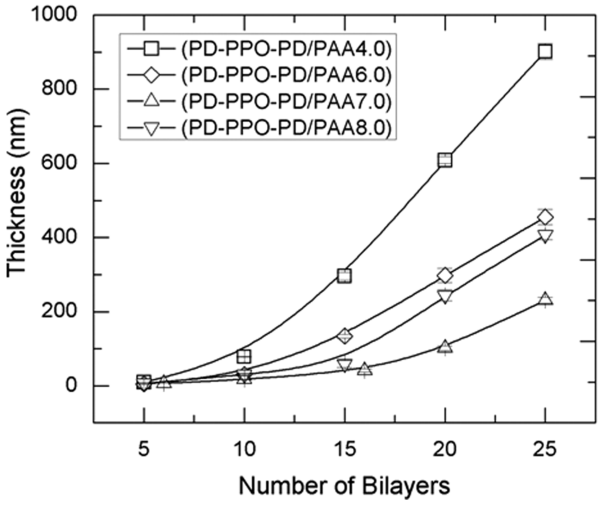

Figure 3. Growth curves obtained for (PD-PPO-PD/PAA4.0), (PD-PPO-PD/PAA6.0), (PD-PPO-PD/PAA7.0), and (PD-PPO-PD/PAA8.0) systems.

3.2.1.2. Layer-by-Layer Assembly of PD-PPO-PD with PAA. In the case of the PD-PPO-PD/PAA multilayer system, exponential growth with large bilayer thickness increments was observed at pH 4. Exponential growth often results from the ability of at least one of the polyelectrolyte components deposited to diffuse into and out of the film during deposition.[68−70] Because AFM studies (data not shown) revealed insignificant changes in surface roughness of these films with bilayer deposition number, exponential growth of PD-PPO-PD/PAA multilayers suggests that large-scale interdiffusion is occurring during the assembly process. This diffusion-enabled exponential growth has been observed in a variety of multilayer systems.[68−71] The weaker ionic bonding between the carboxylic groups on PAA and the charged amine groups on the PD blocks allow interdiffusion of components being deposited into the multilayer. Lynn and coworkers[71] observed exponential growth during the assembly of low-molecular-weight PAA chains with the weak polybase PAH. In our case, however, the molecular weight of the PAA chains is high enough to inhibit diffusion of PAA, suggesting that PD-PPO-PD chains with a low molecular weight of 6200 Da are the diffusing entity. The average per bilayer thickness of 60 nm obtained for (PD-PPO-PD/PAA4.0) is similar to the thickness increments of exponentially growing PAH/low-molecular-weight PAA multilayers previously reported.[71] For the (PD-PPO-PD/PAA7.0) system, linear growth was observed at higher bilayer numbers. The per bilayer thickness increment for the (PD-PPO-PD/PAA7.0) system of ∼20 nm per bilayer is similar to that seen in the all-micelle multilayers.[67]

3.2.2. Effect of pH on the Assembly of the PD-PPO-PD/PAA System. To explore more completely the effect of pH on the growth behavior of the PD-PPO-PD/PAA system, we studied assembly at pH 4, 6, 7, and 8. Figure 3 shows the effect of pH on the assembly of PD-PPO-PD with PAA. The largest overall thickness increments are observed at pH 4, well below the pH at which micelles are formed at RT (∼24 °C). (See Figure 1.)

The pK_a of PAA in the absence of added salt has been reported to be ∼6.5.[72] Therefore, in the pH range of 4−6, the PD-PPO-PD triblock copolymers exist in solution as unimers, and the PAA chains have a degree of ionization that ranges from about 10 to 40% (note: the degree of ionization of a weak polyelectrolyte can change significantly when chains are incorporated into a multilayer).[65,72] Below pH 7, the charge density on PAA increases with increasing solution pH; as such, from pH 4 to 6, the increasing charge density on the PAA chains inhibits this diffusive growth process to some extent, and smaller thickness increments are observed with assembly at pH 6 compared with assembly at pH 4. At both pH 7 and 8, PAA chains are fully charged. Instead, PD-PPO-PD micelles have PD blocks with charge density that decreases with increasing pH. Larger bilayer thickness increments are thus observed at pH 8.

It is noteworthy that the behavior of a polymer chain free in solution often differs from its behavior when adsorbed at a surface. As seen in Figure 1, at 24 °C, solutions of PD-PPO-PD at pH 6 are close to the micellization temperature. Both theoretical[73] and experimental studies[74] indicate that charged amphiphilic block copolymers or surfactants in solutions below their CMC can form micelles at oppositely charged surfaces as the local concentration of charged unimers in the vicinity of an oppositely charged surface exceeds their bulk solution concentration. Because of the similarities in the growth character and swelling behavior (to be discussed) of the (PD-PPO-PD/PAA6.0), (PD-PPO-PD/PAA7.0), and (PD-PPO-PD/PAA8.0), distinct from (PD-PPO-PD/PAA4.0), we believe that micelles were incorporated into multilayers of PD-PPO-PD and PAA assembled at pH 6.

3.2.3. Temperature Response of PD-PPO-PD-Containing Multilayers

3.2.3.1. Effect of PD-PPO-PD Morphology in Solution and Polyanionic Binding Partner on the Swelling of PD-PPO-PD/Polyanion Multilayers. The temperature-dependent swelling of multilayers containing PD-PPO-PD was monitored using in situ ellipsometry. For these experiments, all films were assembled from salt-free solutions at ∼24 °C. By comparing (PD-PPO-PD/PSS7.0), (PD-PPO-PD/PAA7.0), (PD-PPO-PD/PSS4.0), and (PD-PPO-PD/PAA4.0), it is evident from Figure 4 that only multilayers of (PD-PPO-PD/PAA7.0) showed temperature-dependent swelling in DI water adjusted to pH 7. The swelling ratio is defined as a ratio of the ellipsometric thickness of a multilayer in solution to that of a dry film. In the case of the (PD-PPO-PD/PAA7.0), the thickness changes that occurred with changes in temperature were dramatic: the multilayer film thickness increased to 2146 nm (4.11 times its dry thickness of 522 nm) at 6 °C and decreased to 941 nm (1.8 times its dry thickness) at 20 °C.

This dramatic volumetric transition revealed by the sigmoid shaped of the swelling ratio versus temperature plot is a direct consequence of temperature-induced conformational changes in the backbone of PPO that results in a transition from a hydrophilic to a more hydrophobic state as the temperature is raised.[41,75] At 6 °C, the PPO segments are able to hydrogen bond with water molecules, and this association facilitates water uptake and the large degree of swelling at this temperature. Importantly, dissolution does not occur because ionic cross-links between PD and PAA segments remain intact to sustain the network structure in the system. Between 10 and 16 °C, the PPO segments transition into a more hydrophobic form. At 20 °C, PPO is hydrophobic and water is expelled from the PPO micelle cores resulting in the observed deswelling.

In the (PD-PPO-PD/PAA4.0) multilayers, PD-PPO-PD chains were assembled as unimers with the central PPO block forming H bonds with −COOH groups on PAA. Since the temperature-induced swelling response of PPO is dependent on H bond formation between PPO and water molecules at low temperatures, temperature-induced swelling could not be observed in this system where PPO is already H bonded with PAA.

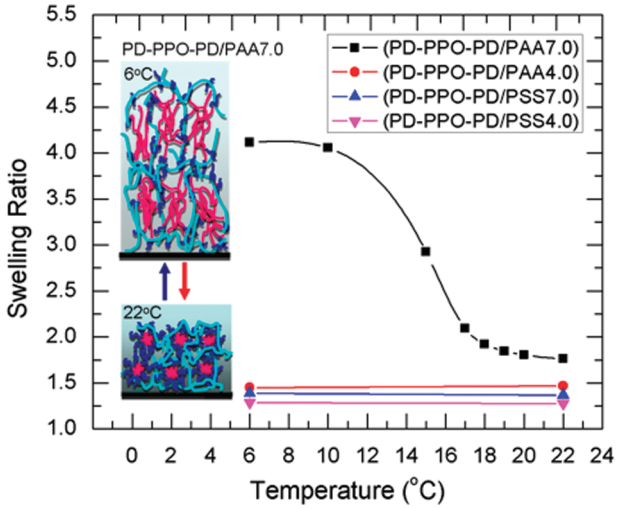

Figure 4. Temperature-dependent swelling of PD-PPO-PD-containing multilayers deposited from solutions, with no added salt, at ~24 °C and subsequently exposed to DI water adjusted to pH 7. Multilayers of PD-PPO-PD were constructed at pH 4 or 7 using PAA or PSS as polyanions. The cartoon illustrates the temperature-induced hydration of micelle cores and thus additional swelling of the (PD-PPO-PD/PAA7.0) multilayer that occurs at low temperature.

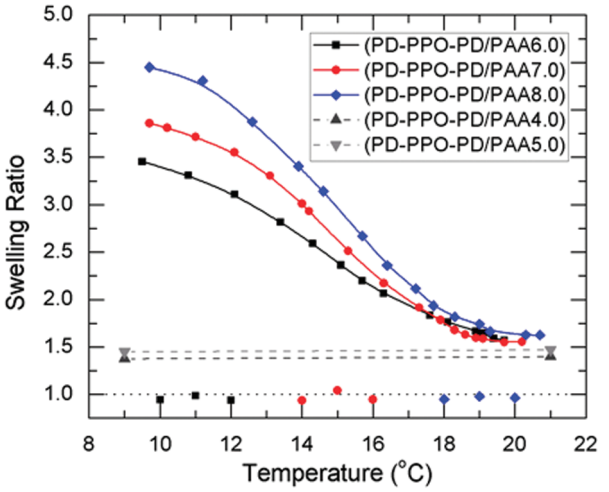

Figure 5. Temperature dependence of swelling of PD-PPO-PD/PAA multilayers assembled from salt-free solutions at pH 6, 7, or 8 submerged in DI adjusted to pH7. Color coded dots around swelling ratio ~1 are the dry film thicknesses after each of three repeated swelling cycles. Swelling of PD-PPO-PD/PAA multilayers assembled at pH 4 and 5 (dashed lines) are included to contrast the lack of temperature-dependent swelling in multilayers assembled at these pH values.

Although micelles are present in the PD-PPO-PD solutions used in the assembly of both (PD-PPO-PD/PSS7.0) and (PD-PPO-PD/PAA7.0) multilayers, a temperature-dependent increase in swelling at low temperatures was not observed in the (PD-PPO-PD/PSS7.0) multilayer. This is a result of the different types of polyanions used in multilayer assembly. PSS and PAA differ in their strength as polyacids and in the stability of the ionic bonds they form within the multilayer: sulfonate-ammonium versus carboxylate-ammonium. As estimated by Dubas et al., the difference in ionic bond strength is ~15 kJ/mol.[76] Ionic cross-links between sulfonate groups on PSS and protonated amine groups on PD, unlike the ionic cross-links between PAA and PD are much stronger and not susceptible to exchange and rearrangement.[76,77] Consequently, (PD-PPO-PD/PSS7.0) films are held together by a tighter network of stronger ionic cross-links.

These results show that the morphology of the block copolymer, the type of bonding that operates within the multilayers, and the density and the nature of ionic bonds between different polyelectrolytes have a profound effect on the resulting molecular architecture of these multilayers and their ability to respond to stimuli.

3.2.3.2. Effect of Assembly pH on the Swelling of PD-PPO-PD/PAA Multilayers. To examine more carefully the effect of assembly pH on the temperature-dependent swelling of PD-PPO-PD/PAA films, we assembled multilayers at pH 5, 6, and 8 in addition to the films assembled at pH 4 and 7. Figure 5 compares the temperature-dependent swelling behavior of PD-PPO-PD/PAA multilayers assembled at different pH when submerged in pH 7 DI water.

A temperature-dependent increase in swelling ratio at low temperature was not observed in multilayers assembled at pH 4 or 5, where unimers were incorporated. The amplitude of the temperature-triggered swelling transition seen in micelle-containing multilayers increased with increasing assembly pH (Figure 5) for (PD-PPO-PD/PAA6.0), (PD-PPO-PD/PAA7.0), and (PD-PPO-PD/PAA8.0) multilayers.

3.2.3.3. Reversibility of Temperature-Triggered Swelling. To harness the temperature-induced volume dilation, the temperature-induced swelling transition has to occur reversibly with high fidelity. Using in situ ellipsometry, the thickness

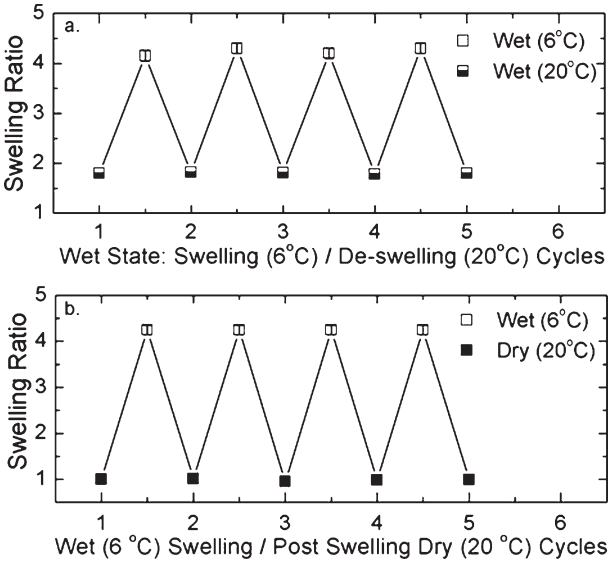

Figure 6. Swelling ratio of $(PD\text{-}PPO\text{-}PD/PAA7.0)_{40}$ multilayer as a function of immersion and drying cycles. (a) Wet-state swelling ratio changes in pH7 DI with temperature cycling between 20 and 6 °C. (b) Changes in the swelling ratio as the film is cycled between the wet (6 °C) swollen state and the dried state after each swelling. No salt was added to these immersion solutions.

of $(PD\text{-}PPO\text{-}PD/PAA7.0)_{40}$ films was monitored over repeated cycles of immersion in DI water adjusted to pH 7 (at 20 or 6 °C) and dried. Wet-state changes in the swelling ratio of a $(PD\text{-}PPO\text{-}PD/PAA7.0)_{40}$ film during cycling between 20 and 6 °C are shown in Figure 6a, whereas the swelling ratio in 6 °C DI water adjusted to pH 7 is contrasted with the dry-state thickness in Figure 6b.

Film swelling/deswelling occurred in a highly reproducible manner (Figure 6a), with negligible film loss over repeated wetting, temperature cycling, and drying cycles (as seen in Figure 6b). The thickness increases and decreases obtained from in situ ellipsometry were accompanied by corresponding decreases and increases in refractive index, indicating that negligible film loss occurred during these cycles.

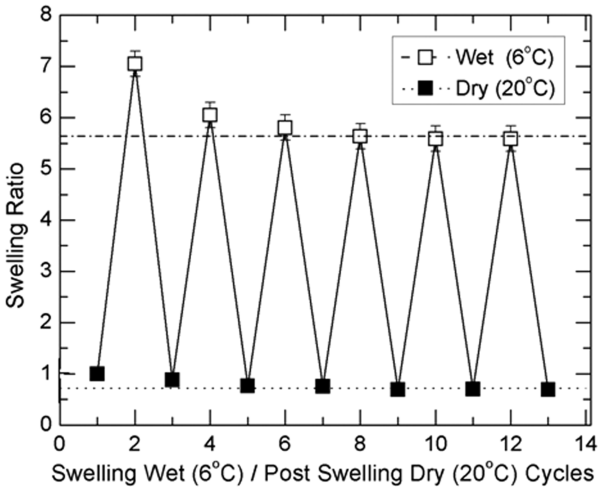

Figure 7. Reversible swelling of $(PD\text{-}PPO\text{-}PD/PAA7.0)_{24}$ multilayers in 0.15 M NaCl solutions at pH 7 (6 °C). The wet-state swollen films are represented by open squares, and the post swelling dried state at 20 °C are represented by filled squares.

3.2.3.4. Effect of Postassembly Salt Concentration and pH on the Swelling of PD-PPO-PD/PAA Multilayers. Because salt is known to destabilize ionic bonding in polyelectrolyte multilayers by competitively binding to charged ionic groups and the screening of charges,[33,77−79] multilayers were tested for stability in 0.15 M NaCl solutions. Salt (0.15 M) was chosen to replicate the ionic strength of physiologically relevant buffers. As demonstrated in Figure 7, the swelling amplitude at 6 °C was higher in 0.15 M NaCl solutions compared with that in salt-free solutions (compare Figures 6 and 7).

This reflects the partial disruption of ionic cross-links within $(PD\text{-}PPO\text{-}PD/PAA7.0)_{24}$ multilayers in salt solutions. Importantly, multilayers remained stable in 0.15 M NaCl solutions, exhibiting reproducible and reversible temperature-dependent swelling responses after some initial densification during the first two cycles. This opens up the possibility of applying these temperature-responsive multilayers in biological systems.

3.2.3.5. Effect of Post-Assembly pH on Film Stability and Swelling of PD-PPO-PD/PAA Multilayers. pH is another important factor that influences the stability of polyelectrolyte multilayers by altering the ratio of positive to negative charges within the multilayer.[33] We studied the effect of immersion solution pH on the swelling of temperature-responsive $(PD\text{-}PPO\text{-}PD/PAA7.0)_{24}$ at both 20 and 6 °C.

Figure 8 shows that at 6 and 20 °C, (PD-PPO-PD/PAA7.0) multilayers are stable and swell reversibly in solutions of pH between 4 and 9. At 20 °C, these films exhibit an approximately constant swelling ratio of ~1.7 independent of the solution pH. Under these conditions, dehydrated hydrophobic PPO domains serve as physical cross-links that help hold the film together and could play a role in opposing increased swelling (observed at 6 °C where the hydrophobic associations between PPO blocks are dissolved) induced by charge imbalances at pH values below or above the deposition pH of 7. At 6 °C, PPO cores in the self-assembled PD-PPO-PD micelles dissolved, causing high, reversible, temperature-induced film swelling in a wide pH range of 4.5 to 8.5. Minimum swelling was observed in DI water at pH 7, the multilayer assembly pH, where the positive and negative charges within the film were balanced. As the immersion solution pH deviated from the assembly pH, additional protonation of the PD and PAA (at lower pH) or deprotonation of PD tertiary amino groups (at higher pH)

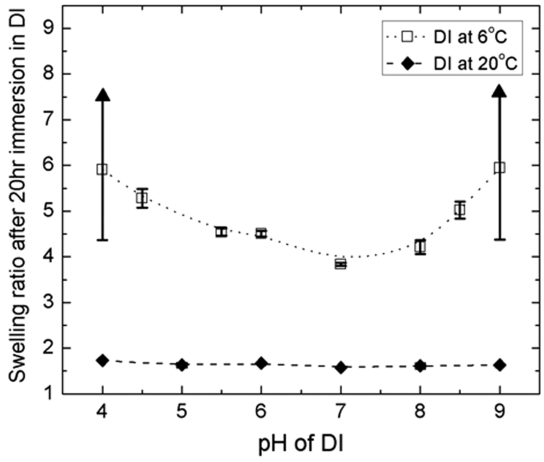

Figure 8. Effect of pH on the swelling of $(PD\text{-}PPO\text{-}PD/PAA7.0)_{24}$ at 20 and 6 °C. At 20 °C (pH < 3 or > 10), as well as at 6 °C (pH < 4.5 or > 8.5), the multilayer films become highly swollen (by a factor of ~7 times or more). For the extreme pH values shown at 6 °C, poor refractive index contrast between highly swollen films and the aqueous medium interfered with obtaining reliable in situ ellipsometric thickness measurements.

resulted in excess positive and negative charge in the film, respectively. The (PD-PPO-PD/PAA7.0) multilayers remained stable after 24 h of immersion at 6 °C in solutions at $3 < pH < 9$, and their swelling was reversible. At 6 °C, pH 4 and 9, because of high (> 85%) water content in the film, the refractive index contrast between the film and water became too low to obtain reliable thickness measurements (indicated by the arrows and large error bars for these points in Figure 8). Finally, films are highly swollen and mechanically weak at extreme pH values < 3 or > 10 at both 6 °C and room temperature of 24 °C, where the majority of ionic associations are disrupted.

4. Conclusions

Triblock copolymers, like PD-PPO-PD, with charged end blocks and a functionality-carrying central block are capable of incorporating novel functionality to electrostatically self-assembled LbL multilayers. We have shown that PD-PPO-PD, a polycationic A-B-A triblock copolymer, can be successfully assembled into multilayers that exhibit reversible temperature-induced swelling and deswelling behavior over a wide range of pH and salt concentrations. As demonstrated here, an understanding of the morphology of the block copolymers being assembled from solution, the charge density of the assembled polyelectrolytes, the LbL assembly mechanism, and the type of bonding involved in the self-assembly process allowed control over the film composition and architecture, which ultimately enabled control over the extent of fully reversible temperature responses. By varying the deposition conditions, we exposed the important factors that enable the stimuli-responsive properties in the multilayer films.

Acknowledgment. This work was partially supported by the MRSEC Program of the National Science Foundation under award number DMR-0819762 and by NSF DMR-0710591 (S. Sukhishvili). We thank the Center for Materials Science and Engineering (CMSE), the Institute for Soldier Nanotechnologies (ISN), and Prof. T. Alan Hatton for use of their characterization facilities.

Supporting Information Available: Micro-DSC data used to estimate the MT of PD-PPO-PD solutions under different pH and salt concentrations, UV−vis spectra of PD-PPO-PD

solutions containing DPH used to infer the CMT, and dynamic light scattering data. This material is available free of charge via the Internet at http://pubs.acs.org.

References and Notes

(1) Gehrke, S. Synthesis, Equilibrium Swelling, Kinetics, Permeability, and Applications of Environmentally Responsive Gels. In *Responsive Gels: Volume Transitions II*; Springer: Berlin, 1993; Vol. *110*, pp 81−144.
(2) Khurma, J. R.; Rohindra, D. R.; Nand, A. V. *Polym. Bull.* **2005**, *54*, 195–204.
(3) Owens, D. E.; Jian, Y.; Fang, J. E.; Slaughter, B. V.; Chen, Y.-H.; Peppas, N. A. *Macromolecules* **2007**, *40*, 7306–7310.
(4) El-Din, H. M. N.; Alla, S. G. A.; El-Naggar, A. W. *J. Macromol. Sci., Part A: Pure Appl. Chem.* **2007**, *44*, 291–297.
(5) Dang, J. M.; Sun, D. D. N.; Shin-Ya, Y.; Sieber, A. N.; Kostuik, J. P.; Leong, K. W. *Biomaterials* **2006**, *27*, 406–418.
(6) Yokota, S.; Matsuyama, K.; Kitaoka, T.; Wariishi, H. *Appl. Surf. Sci.* **2007**, *253*, 5149–5154.
(7) Kwak, D.; Han, J. T.; Lee, J. H.; Lim, H. S.; Lee, D. H.; Cho, K. *Surf. Sci.* **2008**, *602*, 3100–3105.
(8) Nagase, K.; Kobayashi, J.; Okano, T. *J. R. Soc. Interface* **2009**, *6*, S293–S309.
(9) Nü, W.; Yong, Z.; Lei, J. *Macromol. Rapid Commun.* **2008**, *29*, 485–489.
(10) Uto, K.; Yamamoto, K.; Hirase, S.; Aoyagi, T. *J. Controlled Release* **2006**, *110*, 408–413.
(11) Nykanen, A.; Nuopponen, M.; Laukkanen, A.; Hirvonen, S.-P.; Rytela, M.; Turunen, O.; Tenhu, H.; Mezzenga, R.; Ikkala, O.; Ruokolainen, J. *Macromolecules* **2007**, *40*, 5827–5834.
(12) Violet, G.; Havazelet, B.-P. *Biotechnol. Prog.* **2003**, *19*, 1728–1733.
(13) Bromberg, L. E.; Ron, E. S. *Adv. Drug Delivery Rev.* **1998**, *31*, 197–221.
(14) Kuckling, D.; Adler, H.-J. P.; Arndt, K.-F.; Long, L.; Habicher, W. D. *Macromol. Chem. Phys.* **2000**, *201*, 273–280.
(15) Maeda, Y. *Langmuir* **2001**, *17*, 1737–1742.
(16) Lutz, J.-F.; Weichenhan, K.; Akdemir, O.; Hoth, A. *Macromolecules* **2007**, *40*, 2503–2508.
(17) Fournier, D.; Hoogenboom, R.; Thijs, H. M. L.; Paulus, R. M.; Schubert, U. S. *Macromolecules* **2007**, *40*, 915–920.
(18) Decher, G. *Science* **1997**, *277*, 1232–1237.
(19) Stockton, W. B.; Rubner, M. F. *Macromolecules* **1997**, *30*, 2717–2725.
(20) Such, G. K.; Quinn, J. F.; Quinn, A.; Tjipto, E.; Caruso, F. *J. Am. Chem. Soc.* **2006**, *128*, 9318–9319.
(21) Donath, E.; Sukhorukov, G. B.; Caruso, F.; Davis, S. A.; Möhwald, H. *Angew. Chem., Int. Ed.* **1998**, *37*, 2201–2205.
(22) Peyratout, C. S.; Dähne, L. *Angew. Chem., Int. Ed.* **2004**, *43*, 3762–3783.
(23) Sukhorukov, G. B.; Antipov, A. A.; Voigt, A.; Donath, E.; Möhwald, H. *Macromol. Rapid Commun.* **2001**, *22*, 44–46.
(24) Hiller, J. A.; Rubner, M. F. *Macromolecules* **2003**, *36*, 4078–4083.
(25) Kozlovskaya, V.; Sukhishvili, S.A. *Macromolecules* **2006**, *39*, 5569–5572.
(26) Serizawa, T.; Nanameki, K.; Yamamoto, K.; Akashi, M. *Macromolecules* **2002**, *35*, 2184–2189.
(27) Steitz, R.; Leiner, V.; Tauer, K.; Khrenov, V.; v. Klitzing, R. *Appl. Phys. A: Mater. Sci. Process.* **2002**, *74*, s519–s521.
(28) Glinel, K.; Sukhorukov, G. B.; Möhwald, H.; Khrenov, V.; Tauer, K. *Macromol. Chem. Phys.* **2003**, *204*, 1784–1790.
(29) Serpe, M. J.; Jones, C. D.; Lyon, L. A. *Langmuir* **2003**, *19*, 8759–8764.
(30) Nolan, C. M.; Serpe, M. J.; Lyon, L. A. *Biomacromolecules* **2004**, *5*, 1940–1946.
(31) Serpe, M. J.; Yarmey, K. A.; Nolan, C. M.; Lyon, L. A. *Biomacromolecules* **2005**, *6*, 408–413.
(32) Jaber, J. A.; Schlenoff, J. B. *Macromolecules* **2005**, *38*, 1300–1306.
(33) Kharlampieva, E.; Sukhishvili, S. A. *Langmuir* **2003**, *19*, 1235–1243.
(34) Quinn, J. F.; Caruso, F. *Langmuir* **2004**, *20*, 20–22.
(35) Zhu, Z.; Sukhishvili, S. A. *ACS Nano* **2009**, *3*, 3595–3605.
(36) Swiston, A. J.; Cheng, C.; Um, S. H.; Irvine, D. J.; Cohen, R. E.; Rubner, M. F. *Nano Lett.* **2008**, *8*, 4446–4453.
(37) Zhuk, A.; Pavlukhina, S.; Sukhishvili, S. A. *Langmuir* **2009**, *25*, 14025–14029.
(38) Chen, G.; Hoffman, A. S. *Macromol. Rapid Commun.* **1995**, *16*, 175–182.
(39) Bromberg, L. *J. Phys. Chem. B* **1998**, *102*, 10736–10744.
(40) Kell, M. *J. Phys.: Condens. Matter* **1996**, A103.
(41) Linse, P. *J. Phys. Chem.* **2002**, *97*, 13896–13902.
(42) Mortensen, K.; Pedersen, J. S. *Macromolecules* **1993**, *26*, 805–812.
(43) Mortensen, K. *J. Phys.: Condens. Matter* **1996**, *8*, A103–A124.
(44) Su, Y.-l.; Wang, J.; Liu, H.-z. *Macromolecules* **2002**, *35*, 6426–6431.
(45) Lowe, A. B.; Billingham, N. C.; Armes, S. P. *Macromolecules* **1998**, *31*, 5991–5998.
(46) Lin, S.; Du, F.; Wang, Y.; Ji, S.; Liang, D.; Yu, L.; Li, Z. *Biomacromolecules* **2008**, *9*, 109–115.
(47) Baines, F. L.; Armes, S. P.; Billingham, N. C.; Tuzar, Z. *Macromolecules* **1996**, *29*, 8151–8159.
(48) Lee, A. S.; Gast, A. P.; Butun, V.; Armes, S. P. *Macromolecules* **1999**, *32*, 4302–4310.
(49) Bütün, V.; Armes, S. P.; Billingham, N. C. *Polymer* **2001**, *42*, 5993–6008.
(50) Ni, P.-H.; Pan, Q.-S.; Elaïssari, L.-S. Z. C.-C. W. A.; Fu, S.-K. *J. Polym. Sci., Part A: Polym. Chem.* **2002**, *40*, 624–631.
(51) Petrov, P.; Tsvetanov, C. B.; Jerome, R. *J. Phys. Chem. B* **2009**, *113*, 7527–7533.
(52) Lee, D.; Rubner, M. F.; Cohen, R. E. *Nano Lett.* **2006**, *6*, 2305–2312.
(53) Alexandridis, P.; Holzwarth, J. F.; Hatton, T. A. *Macromolecules* **1994**, *27*, 2414–2425.
(54) Schild, H. G.; Tirrell, D. A. *J. Phys. Chem.* **1990**, *94*, 4352–4356.
(55) Ballerat-Busserolles, K.; Rassinoux, S.; Roux-Desgranges, G.; Roux, A. *J. Therm. Anal. Calorim.* **1998**, *51*, 161–171.
(56) Wang, Q.; Li, L.; Jiang, S. *Langmuir* **2005**, *21*, 9068–9075.
(57) Zhou, Y.; Jiang, K.; Song, Q.; Liu, S. *Langmuir* **2007**, *23*, 13076–13084.
(58) Wanka, G.; Hoffmann, H.; Ulbricht, W. *Macromolecules* **1994**, *27*, 4145–4159.
(59) Plamper, F. A.; Ruppel, M.; Schmalz, A.; Borisov, O.; Ballauff, M.; Muller, A. H. E. *Macromolecules* **2007**, *40*, 8361–8366.
(60) Gaisford, S.; Beezer, A. E.; Mitchell, J. C.; Bell, P. C.; Fakorede, F.; Finnie, J. K.; Williams, S. J. *Int. J. Pharm.* **1998**, *174*, 39–46.
(61) An, S. W.; Thomas, R. K.; Baines, F. L.; Billingham, N. C.; Armes, S. P.; Penfold, J. *Macromolecules* **1998**, *31*, 7877–7885.
(62) Lee, A. S.; Butun, V.; Vamvakaki, M.; Armes, S. P.; Pople, J. A.; Gast, A. P. *Macromolecules* **2002**, *35*, 8540–8551.
(63) Martin, T. J.; Prochazka, K.; Munk, P.; Webber, S. E. *Macromolecules* **1996**, *29*, 6071–6073.
(64) Gohy, J.-F.; Antoun, S.; Jerome, R. *Macromolecules* **2001**, *34*, 7435–7440.
(65) Shiratori, S. S.; Rubner, M. F. *Macromolecules* **2000**, *33*, 4213–4219.
(66) Tsukruk, V. V.; Bliznyuk, V. N.; Visser, D.; Campbell, A. L.; Bunning, T. J.; Adams, W. W. *Macromolecules* **1997**, *30*, 6615–6625.
(67) Qi, B.; Tong, X.; Zhao, Y. *Macromolecules* **2006**, *39*, 5714–5719.
(68) Lavalle, P.; Gergely, C.; Cuisinier, F. J. G.; Decher, G.; Schaaf, P.; Voegel, J. C.; Picart, C. *Macromolecules* **2002**, *35*, 4458–4465.
(69) Picart, C.; Mutterer, J.; Richert, L.; Luo, Y.; Prestwich, G. D.; Schaaf, P.; Voegel, J. C.; Lavalle, P. *Proc. Natl. Acad. Sci. U.S.A.* **2002**, *99*, 12531–12535.
(70) Radeva, T.; Kamburova, K.; Petkanchin, I. *J. Colloid Interface Sci.* **2006**, *298*, 59–65.
(71) Sun, B.; Jewell, C. M.; Fredin, N. J.; Lynn, D. M. *Langmuir* **2007**, *23*, 8452–8459.
(72) Choi, J.; Rubner, M. F. *Macromolecules* **2005**, *38*, 116–124.
(73) Cheng, H.; Olvera de la Cruz, M. *Macromolecules* **2006**, *39*, 1961–1970.
(74) Liu, J.-F.; Ducker, W. A. *J. Phys. Chem. B* **1999**, *103*, 8558–8567.
(75) Hurter, P. N.; Scheutjens, J. M. H. M.; Hatton, T. A. *Macromolecules* **2002**, *26*, 5030–5040.
(76) Dubas, S. T.; Schlenoff, J. B. *Langmuir* **2001**, *17*, 7725–7727.
(77) Sukhishvili, S. A.; Kharlampieva, E.; Izumrudov, V. *Macromolecules* **2006**, *39*, 8873–8881.
(78) Nolte, A. J.; Takane, N.; Hindman, E.; Gaynor, W.; Rubner, M. F.; Cohen, R. E. *Macromolecules* **2007**, *40*, 5479–5486.
(79) Sukhishvili, S. A.; Granick, S. *J. Am. Chem. Soc.* **2000**, *122*, 9550–9551.